

Modelling and Control of Quantum Measurement Induced Backaction in Double Quantum Dots

Wei Cui, *Senior Member, IEEE* and Daoyi Dong, *Senior Member, IEEE*

Abstract—Quantum measurements disturb the quantum system being measured, and this is known as measurement-induced backaction. In this work, we consider a double quantum dot monitored by a nearby quantum point contact where the measurement-induced backaction plays an important role. Taking advantage of the quantum master equation approach, we calculate the tunnelling current, and propose a simple feedback-control law to realize and stabilize the tunnelling current. Theoretical analysis and numerical simulations show that the feedback control law can make the current quickly convergent to the desired value.

Index Terms—Quantum control, quantum measurement, measurement-induced backaction, quantum master equation.

I. INTRODUCTION

Controlling quantum systems is an essential task in many applications including quantum information, atomic physics and molecular chemistry [1], [2], [3], [4], [5], [6]. In contrast to classical systems, where measurements do not alter the state of the system, quantum projective measurement [7], [8], [9] collapses a quantum system into one of its eigenstates in a probabilistic manner: the “measurement-induced backaction” (see, e.g., [10], [11], [12], [13] and references therein). Recent progress in macroscopic quantum manipulation and quantum weak measurements have made it possible to perform experiments in which individual quantum systems can be monitored and feedback-controlled in real time [14], [15], [16], [17]. In this paper, we derive a non-Markovian master equation for a double quantum dot (DQD) [18] monitored by a nearby quantum point contact (QPC) where the measurement-induced backaction plays a significant role. In this master equation, time-dependent coefficients can characterize non-Markovian effects. Furthermore, we consider how to reduce the measurement-induced backaction and improve the quantum measurement efficiency by using quantum control theory [19], [20], [21], [22].

Several strategies [23], [24] have already been proposed to reduce quantum measurement-induced backaction. For example, Wiseman [23] considered the measurement-induced backaction based on quantum trajectory theory. In the case

of damping, the jump operator is not Hermitian, and so the measurements permitted by damping are necessarily quantum-demolition measurements. He proved that by feeding back the measurement result to control the system dynamics, the quantum-demolition measurement can be turned into a quantum-nondemolition measurement [23]. The scheme to reduce and suppress the measurement-induced backaction is to obtain a feedback Hamiltonian based on the measurements on the system. A crucial issue in this approach is the necessity to solve a non-linear equation to find the feedback control law. The authors in [24] used measurement and feedback control to attempt to correct the state of the qubit. They demonstrated that projective measurements are not optimal for this task, and that there exists a nonprojective measurement with an optimal measurement strength which achieves the best trade-off between gaining information about the system and disturbing it through measurement backaction. Similar to [23], the feedback control is a unitary rotation whose angle depends on the measurement result.

DQD has been considered as a promising candidate of solid state qubits for quantum computation. This system can be monitored by coupling it to a nearby biased quantum point contact. It is interesting to understand the backaction disturbance resulting from such a detection approach. For a zero-bias DQD, the effect of charge-detector-induced backaction was theoretically studied to explain experimental observations of inelastic electron tunneling [25], [26]. Ref. [27] exposed that under certain conditions the QPC-induced backaction has profound effects on the counting statistics, e.g., changing the shot noise from being sub-Poissonian to super-Poissonian, and changing the skewness from positive to negative. However, how to effectively reduce this measurement-induced backaction is still an open question. Two possible ways have been proposed to reduce the backaction effects by making use of this interference: 1) turn the DQD to an operating point where destructive interference suppresses phonon absorption, and 2) manipulate the electron-phonon interaction. There are various limitations on the applications of these existing strategies [23]. First, it is difficult to estimate quantum states and the measurement-induced backaction from incomplete measurement data. Second, the system of interest is generally open, which means that the dynamics of its environment will affect its evolution. Thus, an accurate master equation is needed to characterize the whole measurement model.

In this paper, a non-Markovian master equation for a DQD monitored by a nearby QPC is derived [28]. Based on an ensemble description of the system of interest, we consider the quantum detection over many identical systems simulta-

This work was supported by the National Natural Science Foundation of China under Grant 11404113, the Australian Research Council's Discovery projects funding scheme under Project DP130101658, and the Guangzhou Key Laboratory of Brain Computer Interaction and Applications under Grant 201509010006.

W. Cui is with the School of Automation Science and Engineering, South China University of Technology, Guangzhou 510641, China (e-mail: aucuiwei@scut.edu.cn).

D. Dong is with the School of Engineering and Information Technology, University of New South Wales, Canberra, ACT 2600, Australia (e-mail: daoyidong@gmail.com).

neously. Moreover, we develop a simple feedback control strategy based on counting statistics to estimate and compensate the measurement-induced backaction in the DQD.

This paper is organized as follows. In Section II we describe a model of a double quantum dot measured by a nearby quantum point contact. Using the quantum master equation, the tunnelling current is calculated in Section III. In Section IV, we design a feedback controller to realize and stabilize a target tunnelling current. Conclusions are given in Section V.

II. PHYSICAL SYSTEM

DQD has been considered as a promising candidate to prepare solid state qubits for quantum computation [29], [30], [31]. This system can be monitored by a nearby QPC and controlled by electronic signals or picosecond laser pulses [32], [33]. The measurement mechanism can be understood as follows. QPC measurements rely on the Coulomb interaction between the DQD and the QPC. The current in the QPC is sensitive to the charge state of the DQD. By measuring the current passing through the QPC one can infer the quantum state of the DQD. However, the measurement-induced backaction will collapse the quantum state. Theoretical and experimental results demonstrated that the backaction of the QPC on the DQD leads to a quantum limit of detection and decoherence [34].

We consider a DQD in the Coulomb-blockade regime with strong intradot and interdot interaction (see Fig. 1(a)). The Hilbert space of the DQD system spanned by three states $|0\rangle$, $|1\rangle$, and $|2\rangle$. Here, the two basis states $|1\rangle \equiv |1, 0\rangle$ and $|2\rangle \equiv |0, 1\rangle$ describe, respectively, one additional electron in the left and right dot above the empty state $|0\rangle \equiv |0, 0\rangle$. Accordingly, the current through the QPC switches between these three different values. The total Hamiltonian of the DQD system is

$$H_0 = H_{\text{DQD}} + H_{\text{Leads}} + H_{\text{T}}, \quad (1)$$

where the dynamics of the interdot DQD system is described by the Hamiltonian ($\hbar = 1$),

$$H_{\text{DQD}} = \epsilon_1 d_1^\dagger d_1 + \epsilon_2 d_2^\dagger d_2 + \Omega(d_1^\dagger d_2 + d_2^\dagger d_1). \quad (2)$$

Here, ϵ_i ($i = 1, 2$) are the energies for a single electron state in each dot, d_i^\dagger is the transpose and conjugate of d_i , Ω is the coupling strength between the two dots, and d_i (d_i^\dagger) represents the electron annihilation (creation) operator in each dot. This system can be approximated as a two-level system, and it is characterized by the energy offset, $\epsilon = \epsilon_2 - \epsilon_1$. The effective Hamiltonian can be written as

$$H_{\text{DQD}} = \frac{\epsilon}{2} \sigma_z + \Omega \sigma_x \quad (3)$$

where $\sigma_z = d_2^\dagger d_2 - d_1^\dagger d_1$ and $\sigma_x = d_2^\dagger d_1 + d_1^\dagger d_2$ are the Pauli matrices for the pseudospin bases of $|1\rangle$ and $|2\rangle$. By diagonalizing the DQD Hamiltonian, we can rewrite it as

$$H_{\text{DQD}} = \omega_0(|e\rangle\langle e| - |g\rangle\langle g|)/2 = \omega_0 \varrho_z/2, \quad (4)$$

where $\varrho_z = |e\rangle\langle e| - |g\rangle\langle g|$, and the eigenstates are

$$|g\rangle = \alpha|1\rangle - \beta|2\rangle,$$

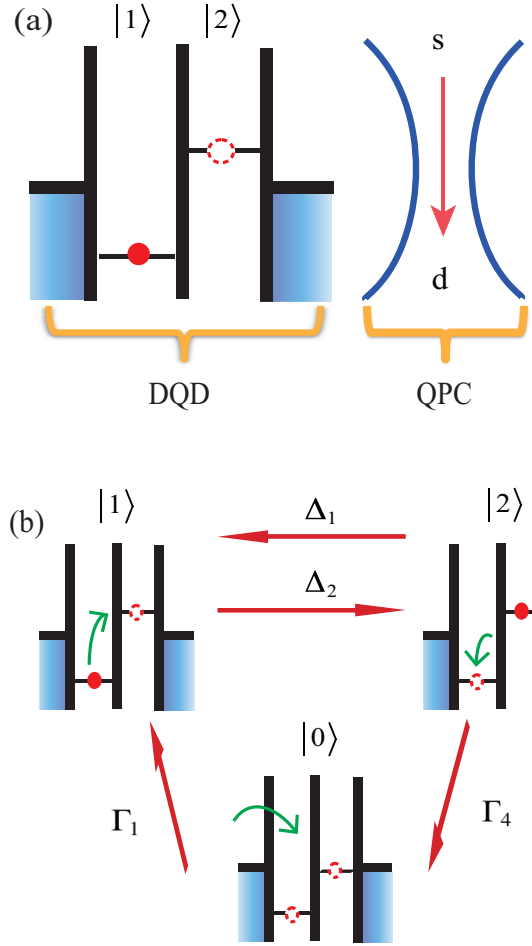


Fig. 1. (a) Schematic diagram of a double quantum dot (DQD) measured by a nearby quantum point contact. The s and d in the QPC denote the source and the drain. (b) Energy-level diagrams for the three states of the DQD. The arrows represent the directions of the electron transitions. The tunnelling rates $\Gamma_{1,4}$ are defined in Eq. (35). The decay rates $\Delta_{1,2}$ are defined in Eq. (36).

$$|e\rangle = \beta|1\rangle + \alpha|2\rangle,$$

with $\alpha \equiv \cos(\theta/2)$, and $\beta \equiv \sin(\theta/2)$. Here θ is given by $\tan \theta = 2\Omega/\epsilon$. The coherent oscillations of the system have a frequency $\omega_0 = \sqrt{\epsilon^2 + 4|\Omega|^2}$.

The Hamiltonian of the two electrodes in the DQD is

$$H_{\text{Leads}} = \sum_k \epsilon_{lk} c_{lk}^\dagger c_{lk} + \epsilon_{rk} c_{rk}^\dagger c_{rk}, \quad (5)$$

where c_{lk} (c_{rk}) is the annihilation operator of an electron in the left (right) lead with quantum numbers k , and ϵ_{lk} (ϵ_{rk}) is the energy of the annihilation operator c_{lk} (c_{rk}). The tunneling Hamiltonian of the DQD and the two electrodes is

$$H_{\text{T}} = \sum_k \left(\Omega_{lk} c_{lk} d_1^\dagger + \Omega_{rk} c_{rk}^\dagger \Lambda_r^\dagger d_2 + \Omega_{lk}^* c_{lk}^\dagger d_1 + \Omega_{rk} c_{rk} \Lambda_r d_2^\dagger \right), \quad (6)$$

which depends on the tunneling coupling strengths Ω_{lk} and Ω_{rk} . Here, Λ_r^\dagger is the operator to count the number of tunnelled electrons [25]. The behavior of the DQD tunnelling process is schematically depicted in Fig. 1(b).

The DQD is measured by a low-transparency QPC, and the total Hamiltonian of this composite system is

$$H_{\text{tot}} = H_0 + H_{\text{QPC}} + H_{\text{int}}, \quad (7)$$

where the Hamiltonians of the QPC and the DQD-QPC interaction are

$$H_{\text{QPC}} = \sum_m \epsilon_{sm} a_{sm}^\dagger a_{sm} + \sum_n \epsilon_{dn} a_{dn}^\dagger a_{dn}, \quad (8)$$

$$H_{\text{int}} = \sum_{m,n} (D - \chi_1 d_1^\dagger d_1 - \chi_2 d_2^\dagger d_2) (a_{sm}^\dagger a_{dn} + a_{dn}^\dagger a_{sm}). \quad (9)$$

Here a_{sm} (a_{dn}) is the electron annihilation operator for electrons in the source (drain) of the QPC with momentum m (n), and ϵ_{sm} (ϵ_{dn}) is the corresponding energy. When a QPC is placed near a DQD, it can be used as an ideal detector to implement quantum weak measurements on the DQD, where the tunnelling barrier of the QPC is modulated by the charge in the nearby DQD. In Eq. (9), D is the tunnelling amplitude of an isolated QPC, χ_1 (χ_2) provides the variation in the tunnelling amplitude when the extra electron stays at the first (second) dot. We assume $\chi_1 < \chi_2$, because the QPC is located closer to the second dot. The current through the QPC is sensitive to the electron location and switches between three values corresponding to the three charge states of the DQD. Figure 1(b) depicts the electron tunnelling in different directions. The current in the QPC allows to obtain quantum state information on the DQD [35].

III. NON-MARKOVIAN MASTER EQUATION

Quantum master equation approach [36] provides a theoretical tool to understanding the dynamics of open quantum systems. In the high-bias case, the behavior of the system density matrix can be described with a master equation of the Lindblad form [25], [27], [34], [37]. In the interaction picture with respect to

$$H' = H_{\text{DQD}} + H_{\text{QPC}},$$

the quantum system is governed by

$$\dot{\rho}_s(t) = - \int_0^t dt' \text{Tr}_E \left[[\rho_s(t) \otimes \rho_E, H_I(t')], H_I(t) \right], \quad (10)$$

where Tr_E indicates the trace over the environmental degrees of freedom, ρ_E is the state of the environment and ρ_s is the system state. The commutator $[\cdot, \cdot]$ is defined by $[A, B] = AB - BA$. The DQD interacts with two environments: the QPC and two electrodes. Thus, the interaction Hamiltonian is [25]

$$H_I(t) = A(t)Y(t) + H_T(t). \quad (11)$$

The first term of the right hand side of Eq. (11) is the interaction with the QPC and

$$\begin{aligned} A(t) &= e^{iH_{\text{DQD}}t} (D - \chi_1 d_1^\dagger d_1 - \chi_2 d_2^\dagger d_2) e^{-iH_{\text{DQD}}t} \\ &= \sum_{j=1}^3 P_j e^{-i\omega_j t} \end{aligned} \quad (12)$$

$$Y(t) = \sum_{m,n} a_{sm}^\dagger a_{dn} e^{i(\epsilon_{sm} - \epsilon_{dn})t} + a_{sm} a_{dn}^\dagger e^{-i(\epsilon_{sm} - \epsilon_{dn})t} \quad (13)$$

with

$$\begin{aligned} P_1 &= -\alpha\beta \chi_d \sigma_+ \\ P_2 &= -\alpha\beta \chi_d \sigma_- \\ P_3 &= D - (\chi_1 |e\rangle\langle e| + \chi_2 |g\rangle\langle g|) + \alpha^2 \chi_d \varrho_z, \end{aligned}$$

and $\omega_1 = -\omega_2 = -\omega_0$, $\omega_3 = 0$, $\chi_d = \chi_1 - \chi_2$. Here $H_T(t)$ describes the interaction with the two leads in the Heisenberg picture,

$$\begin{aligned} H_T(t) &= \sum_k \left[\Omega_{lk} c_{lk} e^{-i\epsilon_{lk}t} (\alpha a_g^\dagger e^{i\omega_0 t} + \beta a_e^\dagger e^{i\omega_0 t}) \right. \\ &\quad + \Omega_{rk} c_{rk}^\dagger e^{i\epsilon_{rk}t} \Lambda_r^\dagger (-\beta a_g e^{-i\omega_0 t} + \alpha a_e e^{-i\omega_0 t}) \\ &\quad + \Omega_{lk}^* c_{lk}^\dagger e^{i\epsilon_{lk}t} (\alpha a_g e^{-i\omega_0 t} + \beta a_e e^{-i\omega_0 t}) \\ &\quad \left. + \Omega_{rk}^* c_{rk} e^{-i\epsilon_{rk}t} \Lambda_r (-\beta a_g^\dagger e^{i\omega_0 t} + \alpha a_e^\dagger e^{i\omega_0 t}) \right] \end{aligned} \quad (14)$$

where $a_g = |0\rangle\langle g|$ and $a_e = |0\rangle\langle e|$ are defined by $d_1^\dagger = |1\rangle\langle 0| = \alpha a_g^\dagger + \beta a_e^\dagger$. The above results can also be found in Ref. [25]. We will use them to derive the dynamic model in this paper.

We first consider the interaction of the DQD with the QPC. Applying Eq. (12) and Eq. (13) to the master equation (10), one obtains

$$\begin{aligned} \dot{\rho}_s(t) &= \int_0^t dt' \left\{ \text{Tr}_E [Y(t') \rho_E Y(t)] \times \right. \\ &\quad \left[A(t') \rho_s(t) A(t) + A(t) \rho_s(t) A(t') \right] - \text{Tr}_E [Y(t) Y(t') \rho_E] \\ &\quad \left[A(t) A(t') \rho_s(t) + \rho_s A(t') A(t) \right] \Big\}, \end{aligned} \quad (15)$$

where

$$\begin{aligned} A(t') \rho_s A(t) &= P_2 \rho_s P_1 e^{i\omega_0(t-t')} + P_1 \rho_s P_2 e^{i\omega_0(t'-t)} \\ &\quad + P_1 \rho_s P_1 e^{i\omega_0(t+t')} + P_2 \rho_s P_2 e^{-i\omega_0(t+t')} \\ &\quad + P_3 \rho_s P_1 e^{i\omega_0 t} + P_3 \rho_s P_2 e^{-i\omega_0 t} \\ &\quad + P_1 \rho_s P_3 e^{i\omega_0 t'} + P_2 \rho_s P_3 e^{-i\omega_0 t'} \\ &\quad + P_3 \rho_s P_3 \end{aligned} \quad (16)$$

and

$$\begin{aligned} A(t) A(t') \rho_s &= P_1 P_2 \rho_s e^{i\omega_0(t-t')} + P_2 P_1 \rho_s e^{i\omega_0(t'-t)} \\ &\quad + P_1 P_1 \rho_s e^{i\omega_0(t+t')} + P_2 P_2 \rho_s e^{-i\omega_0(t+t')} \\ &\quad + P_1 P_3 \rho_s e^{i\omega_0 t} + P_2 P_3 \rho_s e^{-i\omega_0 t} \\ &\quad + P_3 P_1 \rho_s e^{i\omega_0 t'} + P_3 P_2 \rho_s e^{-i\omega_0 t'} \\ &\quad + P_3 P_3 \rho_s. \end{aligned} \quad (17)$$

To simplify the notation, we ignore the subscript s (for system, not source). Neglecting the fast-oscillating terms, we obtain the master equation:

$$\begin{aligned} \dot{\rho} &= \Gamma_+(t) (P_2 \rho P_1 - P_1 P_2 \rho) + \Gamma_-(t) (P_1 \rho P_2 - P_2 P_1 \rho) \\ &\quad + \Gamma'_+(t) (P_1 \rho P_2 - \rho P_2 P_1) + \Gamma'_-(t) (P_2 \rho P_1 - \rho P_1 P_2) \\ &\quad + \Lambda(t) (P_3 \rho P_3 - P_3 P_3 \rho) + \Lambda'(t) (P_3 \rho P_3 - \rho P_3 P_3), \end{aligned} \quad (18)$$

where

$$\begin{aligned}\Gamma_{\pm}(t) &= \int_0^t \langle Y(s)Y(0) \rangle \exp(\pm i\omega_0 s) ds \\ \Gamma'_{\pm}(t) &= \int_0^t \langle Y(0)Y(s) \rangle \exp(\pm i\omega_0 s) ds \\ \Lambda(t) &= \int_0^t \langle Y(s)Y(0) \rangle ds \\ \Lambda'(t) &= \int_0^t \langle Y(0)Y(s) \rangle ds.\end{aligned}\quad (19)$$

Here, we define $t - t' \equiv s$ and

$$\text{Tr}_E\{Y(t)Y(t')\rho_E\} \equiv \langle Y(s)Y(0) \rangle.$$

Note that the two-time reservoir correlation function $\langle Y(s)Y(0) \rangle$ is

$$\begin{aligned}\langle Y(s)Y(0) \rangle &= \sum_{mm'nn'} \langle Y_{m,n}(s)Y_{m',n'}(0) \rangle \delta_{m,m'} \delta_{n,n'} \\ &= \sum_{mn} N_{sm}(1 - N_{dn}) e^{i(\epsilon_{sm} - \epsilon_{dn})s} \\ &\quad + (1 - N_{sm})N_{dn} e^{-i(\epsilon_{sm} - \epsilon_{dn})s}.\end{aligned}\quad (20)$$

The notation $\langle \dots \rangle$ stands for the statistical average over the source and the drain reservoirs of the QPC. They are assumed to be in thermal equilibrium with the Fermi-Dirac distribution function

$$N_{sm} = \left\{ \exp \left[\frac{(\epsilon_{sm} - \mu_s)}{k_B T} \right] + 1 \right\}^{-1}, \quad (21)$$

$$N_{dn} = \left\{ \exp \left[\frac{(\epsilon_{dn} - \mu_d)}{k_B T} \right] + 1 \right\}^{-1}, \quad (22)$$

where $\mu_s = \mu_F \pm eV_{\text{QPC}}/2$ and $\mu_d = \mu_F \pm eV_{\text{QPC}}/2$ are the applied QPC bias voltages. Thus, the coefficients (19) become

$$\begin{aligned}\Gamma_{\pm}(t) &= \int_0^t ds \sum_{mn} \left\{ N_{sm}(1 - N_{dn}) \cos(\epsilon_{sm} - \epsilon_{dn} \pm \omega_0)s \right. \\ &\quad + (1 - N_{sm})N_{dn} \cos(\epsilon_{sm} - \epsilon_{dn} \mp \omega_0)s \\ &\quad + i \left[N_{sm}(1 - N_{dn}) \sin(\epsilon_{sm} - \epsilon_{dn} \pm \omega_0)s \right. \\ &\quad \left. \left. - (1 - N_{sm})N_{dn} \sin(\epsilon_{sm} - \epsilon_{dn} \mp \omega_0)s \right] \right\},\end{aligned}\quad (23)$$

$$\begin{aligned}\Gamma'_{\pm}(t) &= \int_0^t ds \sum_{mn} \left\{ N_{sm}(1 - N_{dn}) \cos(\epsilon_{sm} - \epsilon_{dn} \mp \omega_0)s \right. \\ &\quad + (1 - N_{sm})N_{dn} \cos(\epsilon_{sm} - \epsilon_{dn} \pm \omega_0)s \\ &\quad + i \left[-N_{sm}(1 - N_{dn}) \sin(\epsilon_{sm} - \epsilon_{dn} \mp \omega_0)s \right. \\ &\quad \left. \left. + (1 - N_{sm})N_{dn} \sin(\epsilon_{sm} - \epsilon_{dn} \pm \omega_0)s \right] \right\},\end{aligned}\quad (24)$$

$$\begin{aligned}\Lambda(t) &= \int_0^t ds \sum_{mn} \left\{ i(N_{sm} - N_{dn}) \sin(\epsilon_{sm} - \epsilon_{dn})s \right. \\ &\quad \left. + (N_{sm} + N_{dn} - 2N_{sm}N_{dn}) \cos(\epsilon_{sm} - \epsilon_{dn})s \right\},\end{aligned}\quad (25)$$

$$\begin{aligned}\Lambda'(t) &= \int_0^t ds \sum_{mn} \left\{ -i(N_{sm} - N_{dn}) \sin(\epsilon_{sm} - \epsilon_{dn})s \right. \\ &\quad \left. + (N_{sm} + N_{dn} - 2N_{sm}N_{dn}) \cos(\epsilon_{sm} - \epsilon_{dn})s \right\}.\end{aligned}\quad (26)$$

For the sake of simplicity, we define the new variables

$$\omega_m \equiv \epsilon_{sm} - \mu_s \quad (27)$$

$$\omega_n \equiv \epsilon_{dn} - \mu_d. \quad (28)$$

It is clear that

$$\epsilon_{sm} - \epsilon_{dn} = \omega_m - \omega_n + eV_{\text{QPC}}.$$

Thus, the master equation (18) reduces to

$$\begin{aligned}\frac{d}{dt}\rho &= -i \left[\eta \Delta_3(t) \sigma_z + \Delta_5(t) P_3 P_3, \rho_s \right] + \Delta_4(t) \mathcal{D}[P_3] \rho \\ &\quad + \eta \left[\Delta_1(t) + \Delta_2(t) \right] \mathcal{D}[\sigma_+] \rho \\ &\quad + \eta \left[\Delta_1(t) - \Delta_2(t) \right] \mathcal{D}[\sigma_-] \rho.\end{aligned}\quad (29)$$

Now we consider the interaction of the DQD with the two leads. The Hamiltonian of the two electrodes in the DQD is

$$H_{\text{Leads}} = \sum_k \left(\epsilon_{lk} c_{lk}^\dagger c_{lk} + \epsilon_{rk} c_{rk}^\dagger c_{rk} \right), \quad (30)$$

where c_{lk} (c_{rk}) are the annihilation operators of an electron in the left (right) lead with quantum numbers k . The tunnelling Hamiltonian of the DQD and the two electrodes is

$$\begin{aligned}H_T &= \sum_k \left(\Omega_{lk} c_{lk} d_1^\dagger + \Omega_{rk} c_{rk}^\dagger \Lambda_r^\dagger d_2 \right. \\ &\quad \left. + \Omega_{lk} c_{lk}^\dagger d_1 + \Omega_{rk} c_{rk} \Lambda_r d_2^\dagger \right),\end{aligned}\quad (31)$$

which depends on the tunnelling coupling strengths Ω_{lk} and Ω_{rk} . Here, Λ_r^\dagger is the operator used to count the number of electrons that have tunnelled into the right lead. Also, $H_T(t)$ is the interaction with the two leads in the Heisenberg picture as described in (14).

Similarly, using the interaction Hamiltonian $H_T(t)$ in the master equation (10), we obtain the master equation for the system of DQD interacting with the leads (For details, please refer to the Appendix)

$$\begin{aligned}\frac{d}{dt}\rho &= \Gamma_1 \mathcal{D} \left[\alpha a_g^\dagger + \beta a_e^\dagger \right] \rho + \Gamma_2 \mathcal{D} \left[\alpha a_g + \beta a_e \right] \rho \\ &\quad + \Gamma_3 \mathcal{D} \left[\alpha \Lambda_r a_e^\dagger + \beta \Lambda_r a_g^\dagger \right] \rho + \Gamma_4 \mathcal{D} \left[\alpha \Lambda_r^\dagger a_e + \beta \Lambda_r^\dagger a_g \right] \rho.\end{aligned}\quad (32)$$

Now, converting the obtained equation into the Schrödinger picture, we have the master equation as follows

$$\begin{aligned} \frac{d}{dt}\rho = & -i \left[H_{\text{DQD}} + \eta \Delta_3(t) \sigma_z + \Delta_5(t) P_3 P_3, \rho_s \right] \\ & + \Delta_4(t) \mathcal{D}[P_3] \rho + \eta \left[\Delta_1(t) + \Delta_2(t) \right] \mathcal{D}[\sigma_+] \rho \\ & + \eta \left[\Delta_1(t) - \Delta_2(t) \right] \mathcal{D}[\sigma_-] \rho + \Gamma_1 \mathcal{D} \left[\alpha a_g^\dagger + \beta a_e^\dagger \right] \rho \\ & + \Gamma_2 \mathcal{D} \left[\alpha a_g + \beta a_e \right] \rho + \Gamma_3 \mathcal{D} \left[\alpha \Lambda_r a_e^\dagger + \beta \Lambda_r a_g^\dagger \right] \rho \\ & + \Gamma_4 \mathcal{D} \left[\alpha \Lambda_r^\dagger a_e + \beta \Lambda_r^\dagger a_g \right] \rho, \end{aligned} \quad (33)$$

where $\eta = \alpha^2 \beta^2 \chi_d^2$, and the superoperator \mathcal{D} is defined as

$$\mathcal{D}[O]\rho = O\rho O^\dagger - \frac{1}{2}(O^\dagger O\rho + \rho O^\dagger O). \quad (34)$$

The time-dependent parameters in Eq. (33) are

$$\begin{aligned} \Gamma_1 &= \int_0^t \sum_k |\Omega_{l,k}|^2 \left(1 - \tanh \frac{\epsilon_{l,k} - \mu_l}{2k_B T} \right) \cos(\epsilon_{l,k} - \omega_0) s ds \\ \Gamma_2 &= \int_0^t \sum_k |\Omega_{l,k}|^2 \left(1 + \tanh \frac{\epsilon_{l,k} - \mu_l}{2k_B T} \right) \cos(\epsilon_{l,k} - \omega_0) s ds \\ \Gamma_3 &= \int_0^t \sum_k |\Omega_{r,k}|^2 \left(1 - \tanh \frac{\epsilon_{r,k} - \mu_r}{2k_B T} \right) \cos(\epsilon_{r,k} - \omega_0) s ds \\ \Gamma_4 &= \int_0^t \sum_k |\Omega_{r,k}|^2 \left(1 + \tanh \frac{\epsilon_{r,k} - \mu_r}{2k_B T} \right) \cos(\epsilon_{r,k} - \omega_0) s ds, \end{aligned} \quad (35)$$

and additional parameters are given by:

$$\begin{aligned} \Delta_1(t) &= \sum_{mn} \Lambda_1 \int_0^t ds \cos(\omega_m - \omega_n + eV_{\text{QPC}}) s \cos \omega_0 s, \\ \Delta_2(t) &= \sum_{mn} \Lambda_2 \int_0^t ds \sin(\omega_m - \omega_n + eV_{\text{QPC}}) s \sin \omega_0 s, \\ \Delta_3(t) &= \sum_{mn} \Lambda_1 \int_0^t ds \cos(\omega_m - \omega_n + eV_{\text{QPC}}) s \sin \omega_0 s, \\ \Delta_4(t) &= 4 \sum_{mn} \Lambda_1 \int_0^t ds \cos(\omega_m - \omega_n + eV_{\text{QPC}}) s, \\ \Delta_5(t) &= -2 \sum_{mn} \Lambda_2 \int_0^t ds \sin(\omega_m - \omega_n + eV_{\text{QPC}}) s. \end{aligned} \quad (36)$$

The coefficients Λ_1 and Λ_2 are the Fermi functions

$$\begin{aligned} \Lambda_1(\omega_m, \omega_n) &= 1 - \tanh\left(\frac{\omega_m}{2k_B T}\right) \tanh\left(\frac{\omega_n}{2k_B T}\right), \\ \Lambda_2(\omega_m, \omega_n) &= \tanh\left(\frac{\omega_m}{2k_B T}\right) - \tanh\left(\frac{\omega_n}{2k_B T}\right). \end{aligned} \quad (37)$$

In the zero temperature limit ($k_B T = 0$), the functions Λ_1 and Λ_2 reduce to

$$\begin{aligned} \Lambda_1 &= 2 \left| \Theta(\omega_m) - \Theta(\omega_n) \right|, \\ \Lambda_2 &= 2 \left[\Theta(\omega_m) - \Theta(\omega_n) \right], \end{aligned} \quad (38)$$

where Θ is the Heaviside function [36]. Clearly, for different values of ω_m and ω_n , Λ_1 and Λ_2 reduce to different constant values, as shown in Table I.

TABLE I. The Fermi functions Λ_1 and Λ_2 .

ω_m	ω_n	Λ_1	Λ_2
< 0	< 0	0	0
> 0	> 0	0	0
> 0	< 0	2	2
< 0	> 0	2	-2

The master equation obtained in this paper is non-Markovian, but the Born approximation (i.e., second-order perturbation) is still used. The master equation (33) is the result under such an approximation. This is the first main result of this paper. The advantages of this master equation over previous ones are: (i) it has the Lindblad form and the non-Markovian effects are embodied in the time-dependent coefficients, (ii) the tunnelling and decay effect can be clearly understood in the master equation, and (iii) it can be controlled by manipulating the Hamiltonian.

These results are significant because two very different kinds of behaviours, Markovian and non-Markovian, are embodied in these time-dependent coefficients (36). In the zero-temperature limit, the Fermi functions (37) become 0 or ± 2 in certain cases (see Table 1), and the coefficient $\Delta_1(t) - \Delta_2(t)$ of the master equation (33) can be reduced to

$$\begin{aligned} \frac{\Delta_1(t) - \Delta_2(t)}{2} &= \sum_{\omega_m > 0, \omega_n < 0} \frac{\sin(\omega_m - \omega_n + eV_{\text{QPC}} + \omega_0)t}{\omega_m - \omega_n + eV_{\text{QPC}} + \omega_0} t \\ &+ \sum_{\omega_m < 0, \omega_n > 0} \frac{\sin(\omega_m - \omega_n + eV_{\text{QPC}} - \omega_0)t}{\omega_m - \omega_n + eV_{\text{QPC}} - \omega_0} t. \end{aligned} \quad (39)$$

If the coefficient $\Delta_1(t) - \Delta_2(t)$ is positive, the information is always lost during the time evolution of the DQD quantum system. In certain case, the coefficient becomes negative within certain intervals of time, which displays the non-Markovian behaviour. Obviously, in these time intervals, the environment compensates some lost information to the quantum system of interest. The corresponding non-Markovian properties of the negative coefficient were shown in Fig. 1 of Ref. [38]. It is clear that the Markovian dynamics is solely responsible for the long-time limit. We describe the measurement-induced backaction by the tunneling current. We will show that the current is directly determined by the coefficients in Section III. Furthermore, we propose a simple feedback control law to stabilize the current.

IV. MEASUREMENT OUTPUT AND INDUCED BACKACTION

We now investigate electrons tunnelling in the DQD, and use a feedback control method to stabilize a particular current and reduce the measurement-induced backaction. We consider a zero bias across the DQD, and set $\mu_l = \mu_r = 0$. From equation (33) and the following relations [25], [27]

$$\begin{aligned} \langle n | \Lambda_d^\dagger \Lambda_d \rho | n \rangle &= \rho^{(n)}, \\ \langle n | \Lambda_d \Lambda_d^\dagger \rho | n \rangle &= \rho^{(n)}, \\ \langle n | \Lambda_d^\dagger \rho \Lambda_d | n \rangle &= \rho^{(n-1)}, \\ \langle n | \Lambda_d \rho \Lambda_d^\dagger | n \rangle &= \rho^{(n+1)}, \end{aligned} \quad (40)$$

we obtain a n -resolved equation for each reduced density matrix elements:

$$\begin{aligned}\dot{\rho}_{gg}^{(n)} &= \eta \left(\Delta_1 - \Delta_2 \right) \rho_{gg}^{(n)} - \eta \left(\Delta_1 + \Delta_2 \right) \rho_{ee}^{(n)} \\ &\quad + \Gamma_1 \alpha^2 \rho_{00}^{(n)} - \Gamma_4 \beta^2 \rho_{gg}^{(n)}, \\ \dot{\rho}_{ee}^{(n)} &= \eta \left(\Delta_1 + \Delta_2 \right) \rho_{ee}^{(n)} - \eta \left(\Delta_1 - \Delta_2 \right) \rho_{gg}^{(n)} \\ &\quad + \Gamma_1 \beta^2 \rho_{00}^{(n)} - \Gamma_4 \alpha^2 \rho_{ee}^{(n)}, \\ \dot{\rho}_{00}^{(n)} &= -\Gamma_1 \rho_{00}^{(n)} + \Gamma_4 \left(\beta^2 \rho_{gg}^{(n-1)} + \alpha^2 \rho_{ee}^{(n-1)} \right),\end{aligned}\quad (41)$$

where n is the number of electrons that have tunnelled through the DQD via the right tunnelling barrier at time t so that the density matrix elements $\rho_{ij} = \sum_n \rho_{ij}^{(n)}$ ($i, j = 0, g, e$). An electron can tunnel from the left lead into one of the eigenstates $|g\rangle$ and $|e\rangle$ with tunnelling rates $\Gamma_1 \alpha^2$ and $\Gamma_1 \beta^2$, respectively. Later, it may tunnel out of the DQD to the right lead with the rates $\Gamma_4 \beta^2$ from the ground state or $\Gamma_4 \alpha^2$ from the excited state.

Full counting statistics (FCS) has been widely used to analyze this type of phenomena [37], [40], [39]. The FCS method concentrates on the probability distribution for the number of electron tunneling during a given period of time. With the help of FCS, one can extract not only the average or variance, but also higher order moments of electron correlations. This method has also been experimentally verified in detecting the higher-order cumulant of electrical noise [41], [42]. Complete information about the transport properties is contained in the probability distribution

$$P(n, t) = \text{Tr}_s \{ \rho^{(n)}(t) \} = \rho_{00}^{(n)} + \rho_{gg}^{(n)} + \rho_{ee}^{(n)}.$$

We assume that the time period is much larger than the inverse current frequency. This ensures that $n \gg 1$, on average. The corresponding cumulant generating function (CGF) $\mathcal{F}(\zeta, t)$ is [43], [35]

$$\exp[\mathcal{F}(\zeta, t)] = \sum_n P(n, t) \exp(in\zeta), \quad (42)$$

where the auxiliary variable ζ is usually called counting field. The power series expansion of the CGF is:

$$\mathcal{F}(\zeta, t) = \sum_k C_k \frac{(i\zeta)^k}{k!}. \quad (43)$$

It can be proven [43] that every moment of n is finite and $\mathcal{F}(\zeta, t)$ is C^∞ , from which the k th order cumulant is [35], [43]

$$C_k = \left. \frac{\partial^k \mathcal{F}(\zeta, t)}{\partial (i\zeta)^k} \right|_{\zeta \rightarrow 0}. \quad (44)$$

Clearly,

$$\begin{aligned}F(\zeta, t) &= \ln \left(\sum_n P(n, t) e^{in\zeta} \right) \\ &= \ln \left(1 + \sum_{k=1}^{\infty} \frac{(i\zeta)^k}{k!} \langle n^k \rangle \right) \\ &= \nabla_1 - \frac{\nabla_2}{2} + \frac{\nabla_3}{3} - \frac{\nabla_4}{4} + \dots\end{aligned}$$

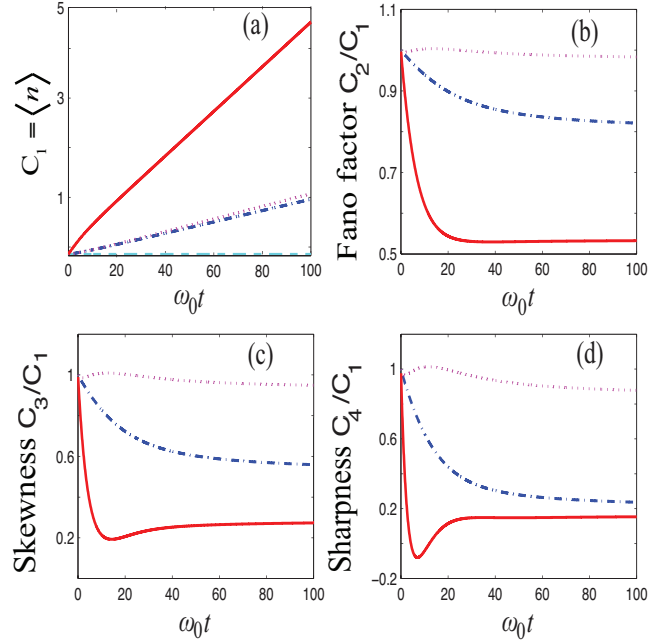


Fig. 2. The mean transport density $C_1 = \langle n \rangle$, the Fano factor C_2/C_1 , the normalized skewness C_3/C_1 , and the normalized sharpness C_4/C_1 versus the detection time for various electron tunneling rates. Here, the cyan-dash lines denote $\Gamma_4 = 0$, the blue-dash-dot lines denote $\Gamma_1 = 0.1, \Gamma_4 = 0.1$, the purple-dot lines denote $\Gamma_1 = 0.5, \Gamma_4 = 0.1$, and the red-solid lines denote $\Gamma_1 = 0.1, \Gamma_4 = 0.5$.

where

$$\langle n^k \rangle = \sum_n n^k P(n, t).$$

When

$$\left| \sum_n P(n, t) (e^{in\zeta} - 1) \right| < 1,$$

one can use the Taylor expansion to derive the cumulants

$$\begin{aligned}\nabla_1 &= (i\zeta) \langle n \rangle + \frac{(i\zeta)^2}{2!} \langle n^2 \rangle + \frac{(i\zeta)^3}{3!} \langle n^3 \rangle + \frac{(i\zeta)^4}{4!} \langle n^4 \rangle + \dots \\ \nabla_2 &= (i\zeta)^2 \langle n \rangle^2 + (i\zeta)^3 \langle n \rangle \langle n^2 \rangle + (i\zeta)^4 \cdot \left(\frac{\langle n^2 \rangle^2}{4} + \frac{2\langle n \rangle \langle n^3 \rangle}{3!} \right) + \dots \\ \nabla_3 &= (i\zeta)^3 \langle n \rangle^3 + (i\zeta)^4 \frac{3\langle n \rangle^2 \langle n^2 \rangle}{2} + \dots \\ \nabla_4 &= (i\zeta)^4 \langle n \rangle^4 + \dots\end{aligned}$$

From Eq. (44), the first four cumulants of the generating function can be expressed as

$$\begin{aligned}C_1(t) &= \langle n \rangle \\ C_2(t) &= \langle n^2 \rangle - \langle n \rangle^2 \\ C_3(t) &= \langle n^3 \rangle - 3\langle n \rangle \langle n^2 \rangle + 2\langle n \rangle^3 \\ C_4(t) &= \langle n^4 \rangle - 3\langle n^2 \rangle^2 - 4\langle n \rangle \langle n^3 \rangle + 12\langle n \rangle^2 \langle n^2 \rangle - 6\langle n \rangle^4.\end{aligned}\quad (45)$$

They denote the mean, variance, asymmetry (“skewness”) and kurtosis (“sharpness”), respectively. The mean transport density $C_1(t)$, the Fano factor C_2/C_1 , the normalized skewness C_3/C_1 , and the normalized sharpness C_4/C_1 are plotted in Fig. 2 for various electron tunneling rates. Here, the cyan-dash lines denote $\Gamma_4 = 0$, the blue-dash-dot lines denote $\Gamma_1 = 0.1, \Gamma_4 = 0.1$, the purple-dot lines denote $\Gamma_1 = 0.5, \Gamma_4 = 0.1$, and the red-solid lines denote $\Gamma_1 = 0.1, \Gamma_4 = 0.5$. The coefficients are set as $\chi_d = 0.5, \epsilon = 108 \mu\text{eV}, \Omega = 32 \mu\text{eV}, V_{\text{QPC}} = 400 \mu\text{eV}$, and the initial condition of Eq. (41) is $\rho_{gg}^{(n)}(0) = \delta_{n,0}$. From Fig. 2(a), we find that if the tunneling rate $\Gamma_4 = 0$, the cumulants will keep zero. If we set $\Gamma_4 = 0.1$ and change Γ_1 from 0.1 to 0.5, there are no significant changes. However, when the tunneling rate of the drain is enhanced to 0.5, drastic changes occur to all the cumulants. The tunnelling current can be extracted from the mean C_1 in Eq. (45),

$$\begin{aligned} I(t) &= e \frac{d}{dt} \langle n \rangle = e \sum_n n \dot{\rho}_n \\ &= e \Gamma_4 \sum_n n \left[\beta^2 (\rho_{gg}^{(n-1)} - \rho_{gg}^{(n)}) + \alpha^2 (\rho_{ee}^{(n-1)} - \rho_{ee}^{(n)}) \right] \\ &= e \Gamma_4 (\beta^2 \rho_{gg}(t) + \alpha^2 \rho_{ee}(t)). \end{aligned} \quad (46)$$

This series is cut-off with $\rho_{gg}^{(-1)} = 0$ and $\rho_{ee}^{(-1)} = 0$, and normalization holds as

$$\sum_n \rho_{gg}^{(n)} = \rho_{gg}$$

and

$$\sum_n \rho_{ee}^{(n)} = \rho_{ee}.$$

It is clear that the current linearly depends on the electron tunneling rate Γ_4 and the population of the quantum state.

In the long-time limit, the stationary current $I_s = I(t \rightarrow \infty)$ reads

$$I_s = \frac{e \Gamma_1 \Gamma_4 (2\beta^2 \chi_d^2 \Delta_2 + \Gamma_4)}{I_1 + I_2}, \quad (47)$$

where

$$\begin{aligned} I_1 &= \Gamma_1 \Gamma_4 \left(\frac{\alpha^2}{\beta^2} + \frac{\beta^2}{\alpha^2} \right) + \Gamma_4^2 - \chi_d^2 \Gamma_4 \Delta_2 (2\alpha^2 - 1), \\ I_2 &= \chi_d^2 (\Gamma_4 (\Delta_1 + 2\Delta_2) + 2\Gamma_4 \Delta_1). \end{aligned}$$

It is clear that the stationary current is determined by the tunneling rates [Γ_1 and Γ_4 , defined in Eq. (35)], the measurement-induced decay rates [Δ_1 and Δ_2 , defined in Eq. (36)] and the coupling strength χ_d^2 . In Fig. 3, we plot the stationary current as a function of the energy detuning ϵ for various values of the coupling strength χ_d^2 and tunnelling rates Γ_4 . In Fig. 3(a), by increasing the coupling strength χ_d , the current resonance becomes asymmetrically broadened a bit and its maximum value decreases. This is because the measurement-induced backaction becomes stronger when χ_d is larger. From Fig. 3(b), we can also find that the current is more significant for a larger tunnelling rate Γ_4 . The reason is that the larger the tunnelling rate the more electrons can tunnel. In this paper, we investigate the backaction by considering the influence

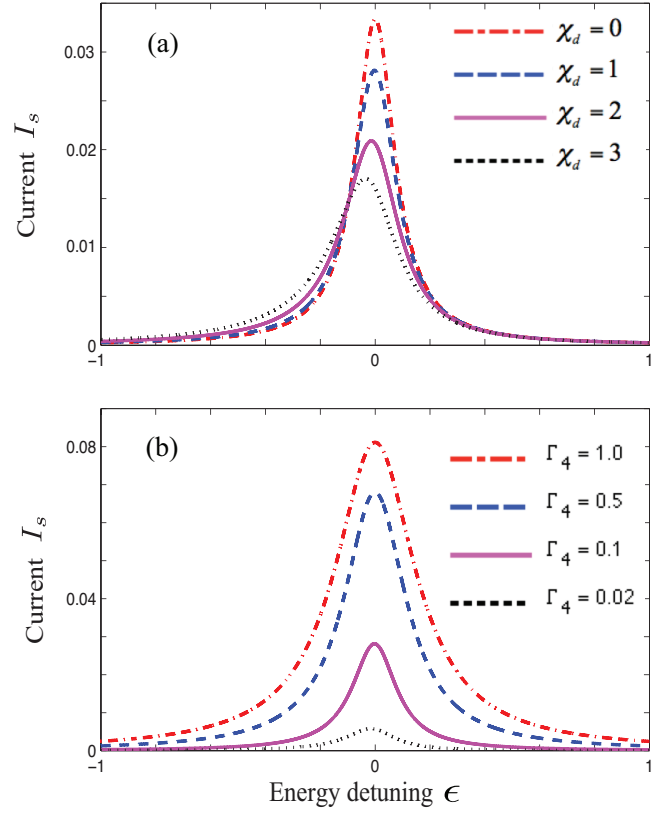


Fig. 3. Stationary transport current I_s as a function of the energy detuning for different parameters. Fig. 3(a) demonstrates that by increasing the coupling strength χ_d , the current resonance becomes asymmetrically broadened a bit and its maximum values decreases; Fig. 3(b) indicates that the current is more significant for a larger tunnelling rate Γ_4 .

of the energy detuning. It is worth noting that recently Ref. [27] demonstrated considerable QPC-induced backaction by investigating the influence of the QPC parameter eV_{QPC} , which is embodied in the decay coefficients of the master equation (33). The authors in [27] showed that when the QPC bias energy eV_{QPC} goes beyond a constant value, the current increases with the magnitude of the voltage applied across the QPC in a nearly linear manner. Here, the energy detuning influence is embedded in the Hamiltonian in the master equation (33). Within this particular structure, the quantum Hamiltonian control method [44] may be used to stabilize a target quantum state and optimize the resulting convergence speed. Below, we use this method to stabilize the tunneling current.

V. STABILIZATION OF THE TUNNELING CURRENT

In this section we specifically study how to stabilize a particular tunneling current. This is similar to tracking control [45] in classical control theory. Feedback is an essential concept in control theory, for its prominent capability in dealing with various uncertainties. In general, quantum semi-classical feedback control consists of applying a conditional Hamiltonian to a quantum system to obtain desired results,

i.e., engineering the system evolution in the form

$$-i \sum_j u_j(t) [H_j, \rho]. \quad (48)$$

The control law $u_j(t)$ is a function of the measurement output

$$u_j(t) = f(t, I(t)). \quad (49)$$

Direct quantum feedback with no time delay is possible if the control is sufficiently strong and fast. In order to obtain a particular tunnelling current, here we design a feedback control law to the double quantum dot. From Eq. (3) there are two adjustable parameters that are experimentally accessible, i.e., the energy level ϵ and the coupling Ω in the system Hamiltonian. We assume that the pulses are ideal and act as an instantaneous unitary operation on the system, so that no coupling to the surroundings needs to be considered during this process. The corresponding system Hamiltonian becomes

$$H'_{\text{DQD}} = \frac{\epsilon + u_1(t)}{2} \sigma_z + [\Omega + u_2(t)] \sigma_x. \quad (50)$$

Explicitly, $u_1(t)$ can be achieved by applying the time-dependent gate voltages on the two dots to vary the level difference between them, and $u_2(t)$ can be achieved by applying a time-dependent gate voltage between the two dots to vary the interdot barrier. Based on the above analysis, we propose a simple feedback control law to realize and stabilize a particular tunnelling current I_0

$$u_i(t) = \text{sgn}[I_0 - I(t)] \eta_i \exp\left(-\frac{1}{k|I_0 - I(t)|}\right), \quad (51)$$

where $\eta_i > 0$ is the control amplitude, $k > 0$ is an adaptive factor, I_0 is the target electron current, and sgn is the sign function,

$$\text{sgn}(x) = \begin{cases} 1 & \text{if } x > 0, \\ 0 & \text{if } x = 0, \\ -1 & \text{if } x < 0. \end{cases} \quad (52)$$

Thus, the tunneling current $I(t)$ in Eq. (51) determines whether to increase or decrease the tunnelling coupling and the energy level (speed up or slow down the electron tunnelling). It is clear that the controller (51) has the characteristics

$$\begin{cases} \lim_{I(t) \rightarrow I_0} u_i(t) = 0, \\ u_i(t) \rightarrow -\eta_i, & \text{if } I(t) \gg I_0, \\ u_i(t) \rightarrow +\eta_i, & \text{if } I(t) \ll I_0. \end{cases} \quad (53)$$

Equation (53) demonstrates that if the current $I(t)$ is smaller than the target one, a stronger coupling strength is applied, which will speed up the electron transport. If the current $I(t)$ is larger than the target one, a weaker coupling strength is applied, which will slow down the electron tunnelling. This algorithm (feedback control process) will end when $I(t) \rightarrow I_0$.

In Fig. 4 we show the numerical results for the current difference $I_0 - I(t)$ as a function of $\omega_0 t$ for various control amplitudes. Here we set $I_0 = 0.1$ and the factor $k = 5 \times 10^4$. Note that all the parameters are dimensionless. It is clear that with the feedback control law, the current $I(t)$ quickly converges to the target value I_0 . It is also demonstrated in

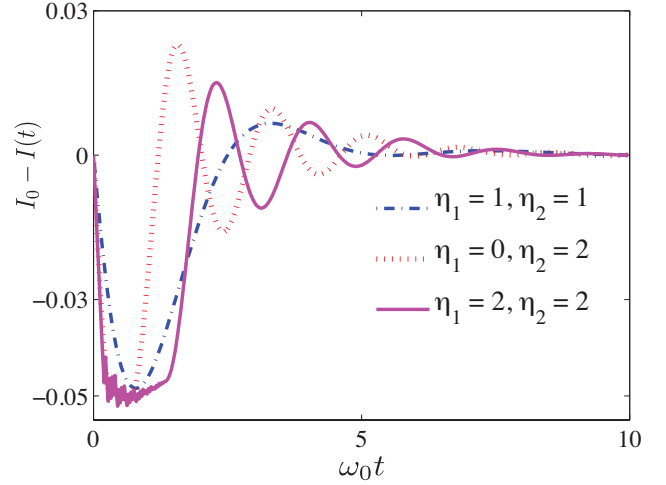


Fig. 4. Current difference, $I_0 - I(t)$ as a function of $\omega_0 t$, for various control amplitudes. The blue dot-dashed line corresponds to $\eta_1 = \eta_2 = 1$, the red dotted line corresponds to $\eta_1 = 0, \eta_2 = 2$, and the purple solid line for $\eta_1 = \eta_2 = 2$. Note that the feedback control law can quickly drive the current $I(t)$ to the expect one I_0 .

Fig. 5 that for various control amplitudes η_i , the behaviours of the feedback controller are quite different. Usually, the larger the amplitude, the more oscillation behaviour. The reason is that the sign function determines whether to increase or decrease the tunnelling coupling and the energy level, the amplitude indicates how large the control law is and the factor indicates how quick the current $I(t)$ convergences to the target value. We consider that the feedback control (30) acts on an ensemble and the measurement is implemented over many identical systems simultaneously. Thanks to the current technology, the measurement and feedback control of a charge qubit in a DQD can be implemented in the experiment; e.g., see [46].

VI. CONCLUSION

We considered the non-Markovian dynamics of open quantum systems and a time-dependent master equation for a DQD interacting with the QPC was derived. We further illustrated several basic features of quantum non-Markovianity by analyzing the first four cumulants. Moreover, we propose a control algorithm to realize and stabilize a particular tunnelling current from its surrounding environment. The strategy can be summarized as follows: we calculate the cumulants of full counting statistics by the master equation, and then deduce the tunnelling current. Based on the tunnelling current, a Hamiltonian feedback control law was proposed to realize and stabilize a particular measurement current. We considered a specific physical set-up of a double quantum dot measured by a nearby quantum point contact. Theoretical analysis and numerical simulations show that the control algorithm can make the current quickly convergent to the target value, and thus enhance the performance of the quantum measurement.

APPENDIX: MASTER EQUATION FOR DQD INTERACTING WITH THE LEADS

Using the interaction Hamiltonian $H_T(t)$ in the master equation (10), we obtain the master equation for the system of DQD interacting with the leads as follows [28]:

$$\dot{\rho} = \alpha^2 \text{I} + \beta^2 \text{II} + \beta^2 \text{III} + \alpha^2 \text{IV}, \quad (54)$$

where

$$\begin{aligned} \text{I} &= \Gamma_{l,-} (a_g^\dagger \rho a_g - a_g a_g^\dagger \rho) + \Gamma'_{l,-} (a_g \rho a_g^\dagger - \rho a_g^\dagger a_g) \\ &\quad + \Gamma_{l,+} (a_g \rho a_g^\dagger - a_g^\dagger a_g \rho) + \Gamma'_{l,+} (a_g^\dagger \rho a_g - \rho a_g a_g^\dagger) \\ &= -i \left[\frac{\Gamma_{l,-} - \Gamma'_{l,+}}{2i} a_g a_g^\dagger - \frac{\Gamma_{l,+} - \Gamma'_{l,-}}{2i} a_g^\dagger a_g, \rho \right] \\ &\quad + (\Gamma_{l,-} + \Gamma'_{l,+}) \mathcal{D}[a_g^\dagger] \rho + (\Gamma_{l,+} + \Gamma'_{l,-}) \mathcal{D}[a_g] \rho, \end{aligned} \quad (55)$$

$$\begin{aligned} \text{II} &= \Gamma_{l,-} (a_e^\dagger \rho a_e - a_e a_e^\dagger \rho) + \Gamma'_{l,-} (a_e \rho a_e^\dagger - \rho a_e^\dagger a_e) \\ &\quad + \Gamma_{l,+} (a_e \rho a_e^\dagger - a_e^\dagger a_e \rho) + \Gamma'_{l,+} (a_e^\dagger \rho a_e - \rho a_e a_e^\dagger) \\ &= -i \left[\frac{\Gamma_{l,-} - \Gamma'_{l,+}}{2i} a_e a_e^\dagger - \frac{\Gamma_{l,+} - \Gamma'_{l,-}}{2i} a_e^\dagger a_e, \rho \right] \\ &\quad + (\Gamma_{l,-} + \Gamma'_{l,+}) \mathcal{D}[a_e^\dagger] \rho + (\Gamma_{l,+} + \Gamma'_{l,-}) \mathcal{D}[a_e] \rho, \end{aligned} \quad (56)$$

$$\begin{aligned} \text{III} &= \Gamma_{r,-} (\Lambda_r a_g^\dagger \rho \Lambda_r^\dagger a_g - \Lambda_r^\dagger a_g \Lambda_r a_g^\dagger \rho) \\ &\quad + \Gamma'_{r,-} (\Lambda_r^\dagger a_g \rho \Lambda_r a_g^\dagger - \rho \Lambda_r a_g^\dagger \Lambda_r^\dagger a_g) \\ &\quad + \Gamma_{r,+} (\Lambda_r^\dagger a_g \rho \Lambda_r a_g^\dagger - \Lambda_r a_g^\dagger \Lambda_r^\dagger a_g \rho) \\ &\quad + \Gamma'_{r,+} (\Lambda_r a_g^\dagger \rho \Lambda_r^\dagger a_g - \rho \Lambda_r^\dagger a_g \Lambda_r a_g^\dagger) \\ &= (\Gamma_{r,-} + \Gamma'_{r,+}) \mathcal{D}[\Lambda_r a_g^\dagger] \rho + (\Gamma_{r,+} + \Gamma'_{r,-}) \mathcal{D}[\Lambda_r^\dagger a_g] \rho \\ &\quad - i \left[\frac{\Gamma_{r,-} - \Gamma'_{r,+}}{2i} \Lambda_r^\dagger a_g \Lambda_r a_g^\dagger, \rho \right] \\ &\quad - i \left[-\frac{\Gamma_{r,+} - \Gamma'_{r,-}}{2i} \Lambda_r a_g^\dagger \Lambda_r^\dagger a_g, \rho \right], \end{aligned} \quad (57)$$

$$\begin{aligned} \text{IV} &= \Gamma_{r,-} (\Lambda_r a_e^\dagger \rho \Lambda_r^\dagger a_e - \Lambda_r^\dagger a_e \Lambda_r a_e^\dagger \rho) \\ &\quad + \Gamma'_{r,-} (\Lambda_r^\dagger a_e \rho \Lambda_r a_e^\dagger - \rho \Lambda_r a_e^\dagger \Lambda_r^\dagger a_e) \\ &\quad + \Gamma_{r,+} (\Lambda_r^\dagger a_e \rho \Lambda_r a_e^\dagger - \Lambda_r a_e^\dagger \Lambda_r^\dagger a_e \rho) \\ &\quad + \Gamma'_{r,+} (\Lambda_r a_e^\dagger \rho \Lambda_r^\dagger a_e - \rho \Lambda_r^\dagger a_e \Lambda_r a_e^\dagger) \\ &= (\Gamma_{r,-} + \Gamma'_{r,+}) \mathcal{D}[\Lambda_r a_e^\dagger] \rho + (\Gamma_{r,+} + \Gamma'_{r,-}) \mathcal{D}[\Lambda_r^\dagger a_e] \rho \\ &\quad - i \left[\frac{\Gamma_{r,-} - \Gamma'_{r,+}}{2i} \Lambda_r^\dagger a_e \Lambda_r a_e^\dagger, \rho \right] \\ &\quad - i \left[-\frac{\Gamma_{r,+} - \Gamma'_{r,-}}{2i} \Lambda_r a_e^\dagger \Lambda_r^\dagger a_e, \rho \right]. \end{aligned} \quad (58)$$

The coefficients are

$$\begin{aligned} \Gamma_{l,-} &= \int_0^t \sum_k |\Omega_{l,k}|^2 \langle c_{l,k}^\dagger c_{l,k} \rangle e^{i(\epsilon_{l,k} - \omega_0)s} ds, \\ \Gamma_{l,+} &= \int_0^t \sum_k |\Omega_{l,k}|^2 \langle c_{l,k} c_{l(r),k}^\dagger \rangle e^{-i(\epsilon_{l,k} - \omega_0)s} ds, \\ \Gamma'_{l,-} &= \int_0^t \sum_k |\Omega_{l,k}|^2 \langle c_{l,k} c_{l,k}^\dagger \rangle e^{i(\epsilon_{l,k} - \omega_0)s} ds, \\ \Gamma'_{l,+} &= \int_0^t \sum_k |\Omega_{l,k}|^2 \langle c_{l,k}^\dagger c_{l,k} \rangle e^{-i(\epsilon_{l,k} - \omega_0)s} ds, \\ \Gamma_{r,-} &= \int_0^t \sum_k |\Omega_{r,k}|^2 \langle c_{r,k}^\dagger c_{r,k} \rangle e^{i(\epsilon_{r,k} - \omega_0)s} ds, \\ \Gamma_{r,+} &= \int_0^t \sum_k |\Omega_{r,k}|^2 \langle c_{r,k} c_{r,k}^\dagger \rangle e^{-i(\epsilon_{r,k} - \omega_0)s} ds, \\ \Gamma'_{r,-} &= \int_0^t \sum_k |\Omega_{r,k}|^2 \langle c_{r,k} c_{r,k}^\dagger \rangle e^{i(\epsilon_{r,k} - \omega_0)s} ds, \\ \Gamma'_{r,+} &= \int_0^t \sum_k |\Omega_{r,k}|^2 \langle c_{r,k}^\dagger c_{r,k} \rangle e^{-i(\epsilon_{r,k} - \omega_0)s} ds, \end{aligned}$$

with the Fermi-Dirac distribution function

$$\begin{aligned} \langle c_{l,k}^\dagger c_{l,k} \rangle &= \left[e^{(\epsilon_{l,k} - \mu_l)/k_B T} + 1 \right]^{-1} \\ &= \frac{1}{2} \left[1 - \tanh \frac{\epsilon_{l,k} - \mu_l}{2k_B T} \right] \end{aligned} \quad (59)$$

and

$$\begin{aligned} \langle c_{r,k}^\dagger c_{r,k} \rangle &= \left[e^{(\epsilon_{r,k} - \mu_r)/k_B T} + 1 \right]^{-1} \\ &= \frac{1}{2} \left[1 - \tanh \frac{\epsilon_{r,k} - \mu_r}{2k_B T} \right]. \end{aligned} \quad (60)$$

Thus, the master equation (54) reduces to

$$\begin{aligned} \frac{d}{dt} \rho &= \Gamma_1 \mathcal{D}[\alpha a_g^\dagger + \beta a_e^\dagger] \rho + \Gamma_2 \mathcal{D}[\alpha a_g + \beta a_e] \rho \\ &\quad + \Gamma_3 \mathcal{D}[\alpha \Lambda_r a_e^\dagger + \beta \Lambda_r a_g^\dagger] \rho + \Gamma_4 \mathcal{D}[\alpha \Lambda_r^\dagger a_e + \beta \Lambda_r^\dagger a_g] \rho, \end{aligned} \quad (61)$$

where

$$\begin{aligned} \Gamma_1 &= \Gamma_{l,-} + \Gamma'_{l,+} \\ &= \int_0^t \sum_k |\Omega_{l,k}|^2 \left(1 - \tanh \frac{\epsilon_{l,k} - \mu_l}{2k_B T} \right) \cos(\epsilon_{l,k} - \omega_0)s ds \\ \Gamma_2 &= \Gamma_{l,+} + \Gamma'_{l,-} \\ &= \int_0^t \sum_k |\Omega_{l,k}|^2 \left(1 + \tanh \frac{\epsilon_{l,k} - \mu_l}{2k_B T} \right) \cos(\epsilon_{l,k} - \omega_0)s ds \\ \Gamma_3 &= \Gamma_{r,-} + \Gamma'_{r,+} \\ &= \int_0^t \sum_k |\Omega_{r,k}|^2 \left(1 - \tanh \frac{\epsilon_{r,k} - \mu_r}{2k_B T} \right) \cos(\epsilon_{r,k} - \omega_0)s ds \\ \Gamma_4 &= \Gamma_{r,+} + \Gamma'_{r,-} \\ &= \int_0^t \sum_k |\Omega_{r,k}|^2 \left(1 + \tanh \frac{\epsilon_{r,k} - \mu_r}{2k_B T} \right) \cos(\epsilon_{r,k} - \omega_0)s ds. \end{aligned} \quad (62)$$

ACKNOWLEDGMENT

The authors would like to thank Prof. Franco Nori and Prof. Jianqiang You for helpful comments.

REFERENCES

- [1] H. M. Wiseman and G. J. Milburn, *Quantum Measurement and Control* Cambridge, Cambridge University Press, 2010.
- [2] D. Dong and I. R. Petersen, "Quantum control theory and applications: A survey," *IET Control Theory & Applications*, vol. 4, no. 12, pp. 2651-2671, 2010.
- [3] D. Dong, M. A. Mabrok, I. R. Petersen, B. Qi, C. Chen, and H. Rabitz, "Sampling-based learning control for quantum systems with uncertainties," *IEEE Transactions on Control Systems Technology*, vol. 23, no. 6, pp. 2155-2166, 2015.
- [4] T. M. Zhang, R.-B. Wu, F. H. Zhang, T. J. Tarn, and G. L. Long, "Minimum-time selective control of homonuclear spins," *IEEE Transactions on Control Systems Technology*, vol. 23, no. 5, pp. 2018-2025, 2015.
- [5] J. Zhang, L. Greenman, X. Deng, K.B. Whaley, "Robust control pulses design for electron shuttling in solid state devices," *IEEE Transactions on Control Systems Technology*, Vol.22, No.6, pp.2354-2359, 2014.
- [6] W. Zhang, D. Dong, and I. R. Petersen, "Adaptive target scheme for learning control of quantum systems," *IEEE Transactions on Control Systems Technology*, in press, DOI: 10.1109/TCST.2017.2715007, 2017.
- [7] J. von Neumann, *Mathematical Foundations of Quantum Mechanics*, Princeton: Princeton University, 1955.
- [8] A. G. Kofman, S. Ashhab, and F. Nori, "Nonperturbative theory of weak pre- and post-selected measurements," *Physics Reports*, vol. 520, no.2, pp. 43-134, 2012.
- [9] K. Jacobs, *Quantum Measurements Theory and Its Application*, Cambridge: Cambridge University, 2014.
- [10] J. Dressel and F. Nori, "Certainty in Heisenberg's uncertainty principle: Revisiting definitions for estimation errors and disturbance," *Physical Review A*, vol. 89, p. 022106, 2014.
- [11] M. Hatridge, S. Shankar, M. Mirrahimi, F. Schackert, K. Geerlings, T. Brecht, K. M. Sliwa, B. Abdo, L. Frunzio, S. M. Girvin, R. J. Schoelkopf, and M. H. Devoret, "Quantum back-action of an individual variable-strength measurement," *Science*, vol. 339, no.6116, pp.178-181, 2013.
- [12] W. Cui, N. Lambert, Y. Ota, X. Y. Lü, Z. L. Xiang, J. Q. You, and F. Nori, "Confidence and backaction in the quantum filter equation," *Physical Review A*, vol. 86, no. 5, p. 052320, 2012.
- [13] M. Kulkarni, O. Cotlet, and H. E. Türeci, "Cavity-coupled double-quantum dot at finite bias: Analogy with lasers and beyond," *Physical Review B*, vol. 90, p. 125402, 2014.
- [14] C. Sayrin, I. Dotsenko, X. Zhou, B. Peaudecerf, T. Rybarczyk, S. Gleyzes, P. Rouchon, M. Mirrahimi, H. Amini, M. Brune, J. M. Raimond, and S. Haroche, "Real-time quantum feedback prepares and stabilizes photon number states," *Nature (London)*, vol. 477, pp. 73-77, 2011.
- [15] H. Yonezawa, D. Nakane, T. A. Wheatley, K. Iwasawa, S. Takeda, H. Argo, K. Ohki, K. Tsumura, D. W. Berry, T. C. Ralph, H. M. Wiseman, E. H. Huntington, and A. Furusawa, "Quantum-enhanced optical-phase tracking," *Science* vol. 337, no.6101, pp. 1514-1517, 2012.
- [16] I. Iida, M. Yukawa M, H. Yonezawa, N. Yamamoto, and A. Furusawa, "Experimental demonstration of coherent feedback control on optical field squeezing," *IEEE Transactions on Automatic Control*, vol. 57, pp. 2045-2050, 2012.
- [17] G. F. Zhang and M. R. James, "Direct and indirect couplings in coherent feedback control of linear quantum systems," *IEEE Transactions on Automatic Control*, vol. 56, pp. 1535-1550, 2011.
- [18] X. Mi, J. V. Cady, D. M. Zajac, J. Stehlik, L. F. Edge, and J. R. Petta, "Circuit Quantum Electrodynamics Architecture for Gate-Defined Quantum Dots in Silicon," *Applied Physics Letters* vol. 110, p. 043502, 2017.
- [19] D. Dong and Ian R. Petersen, "Sliding mode control of two-level quantum systems," *Automatica*, vol. 48, no.5, pp. 725-735, 2012.
- [20] M. R. James and J. E. Gough, "Quantum dissipative systems and feedback control design by interconnection," *IEEE Transactions on Automatic Control*, vol. 55, pp. 1806-1821, no. 8, 2010.
- [21] B. Qi, "A two-step strategy for stabilizing control of quantum systems with uncertainties," *Automatica*, vol. 49, no. 3, pp. 834-839, 2013.
- [22] N. Yamamoto and L. Bouten, "Quantum risk-sensitive estimation and robustness," *IEEE Transactions on Automatic Control*, vol. 54, pp.92-107, 2009.
- [23] H. M. Wiseman, "Using feedback to eliminate back-action in quantum measurements," *Physical Review A*, vol. 51, vol.3, p. 2459, 1995.
- [24] A. M. Brańczyk, P. E. M. F. Mendonça, A. Gilchrist, A. C. Doherty, and S. D. Bartlett, "Unambiguous discrimination of special sets of multipartite states using local measurements and classical communication," *Physical Review A* vol. 75, no. 1, p. 012329, 2007.
- [25] S. H. Ouyang, C. H. Lam, and J. Q. You, "Backaction of a charge detector on a double quantum dot," *Physical Review B*, vol. 81, p. 075301, 2010.
- [26] Z. Z. Li, S. H. Ouyang, C. H. Lam, and J. Q. You, "Probing the quantum behavior of a nanomechanical resonator coupled to a double quantum dot," *Physical Review B*, vol. 85, p. 235420, 2012.
- [27] Z. Z. Li, C. H. Lam, T. Yu, and J. Q. You, "Detector-induced backaction on the counting statistics of a double quantum dot," *Scientific Reports*, vol. 3, p. 3026, 2013.
- [28] W. Cui, "Dynamics of a double quantum dot charge qubit measured by a quantum point contact," *Proceedings of the 34th Chinese Control Conference*, pp. 8281-8286, Hangzhou, China, 28th-30th July 2015.
- [29] B. B. Chen, B. C. Wang, G. Cao, H. O. Li, M. Xiao, G. C. Guo, H. W. Jiang, X. Hu, and G. P. Guo, "Spin blockade and coherent dynamics of high-spin states in a three-electron double quantum dot," *Physical Review B*, vol. 95, p. 035408, 2017.
- [30] A. Stockklauser, P. Scarlino, J. Koski, S. Gasparinetti, C. K. Andersen, C. Reichl, W. Wegscheider, T. Ihn, K. Ensslin, and A. Wallraff, "Strong coupling cavity QED with gate-defined double quantum dots enabled by a high impedance resonator," *Physical Review X*, vol. 7, p. 011030, 2017.
- [31] M. J. A. Schuetz, G. Giedke, L. M. K. Vandersypen, and J. I. Cirac, "High-fidelity hot gates for generic spin-resonator systems," *Physical Review A*, vol. 95, p. 052335, 2017.
- [32] T. Brandes, "Feedback control of quantum transport," *Physical Review Letters* vol. 105, p. 060602, 2010.
- [33] G. G. Gillett, R. B. Dalton, B. P. Lanyon, M. P. Almeida, M. Barbieri, G. J. Pryde, J. L. O'Brien, K. J. Resch, S. D. Bartlett, and A. G. White, "Experimental feedback control of quantum systems using weak measurements," *Physical Review Letters*, vol. 104, p. 080503, 2010.
- [34] X. Q. Li, P. Cui, and Y. J. Yan, "Spontaneous relaxation of a charge qubit under electrical measurement," *Physical Review Letters* vol. 94, p. 066803, 2005.
- [35] C. Pöhl, C. Emary, and T. Brandes, "Feedback stabilization of pure states in quantum transport," *Physical Review B*, vol. 84, p. 085302, 2011.
- [36] H. P. Breuer and F. P. Petruccione, *The Theory of Open Quantum Systems*, Oxford: Oxford University Press, 2002.
- [37] S. A. Gurvitz and Y. S. Prager, "Microscopic derivation of rate equations for quantum transport," *Physical Review B*, vol. 53, p. 15932, 1996.
- [38] W. Cui, Z. R. Xi, and Y. Pan, "Controlled population transfer for quantum computing in non-Markovian noise environment," *Proceedings of the IEEE Conference on Decision and Control and Chinese Control Conference*, pp. 2504-2509, Shanghai, China, 15th-18th December 2009.
- [39] G. Schaller, G. Kiesslich, and T. Brandes, "Transport statistics of interacting double dot systems: Coherent and non-Markovian effects," *Physical Review B*, vol. 80, p. 245107, 2009.
- [40] A. J. Keller, J. S. Lim, D. Sánchez, R. López, S. Amasha, J. A. Katine, H. Shtrikman, and D. Goldhaber-Gordon, "Cotunneling drag effect in Coulomb-coupled quantum dots," *Physical Review Letters*, vol. 117, p. 066602, 2016.
- [41] N. Ubbelohde, C. Fricke, C. Flindt, F. Hohls, and R. J. Haug, "Measurement of finite-frequency current statistics in a single-electron transistor," *Nature Communications*, vol. 3, p. 612, 2012.
- [42] V. F. Maisi, D. Kambly, C. Flindt, and P. Pekola, "Full Counting Statistics of Andreev Tunneling," *Physical Review Letters* vol. 112, p. 036801, 2014.
- [43] A. Braggio, K. König, and R. Fazio, "Full counting statistics in strongly interacting systems: non-Markovian effects," *Physical Review Letters*, vol. 96, p. 026805, 2006.
- [44] F. Ticozzi, R. Lucchese, P. Cappellaro, and L. Viola, "Hamiltonian control of quantum dynamical semigroups: stabilization and convergence speed," *IEEE Transactions on Automatic Control*, vol. 57, pp. 1931-1944, 2012.
- [45] S. Xue, M. R. Hush, and I. R. Petersen, "Feedback tracking control of non-Markovian quantum systems," *IEEE Transactions on Control Systems Technology*, vol. 25, no. 5, pp. 1552-1563, 2017.
- [46] G. Cao, H. O. Li, L. Wang, C. Zhou, M. Xiao, G. C. Guo, H. W. Jiang, and G. P. Guo, "Ultrafast universal quantum control of a quantum-dot charge qubit using Landau-Zener-Stueckelberg interference," *Nature Communications*, vol. 4, p. 1401, 2012.